A molecular diffusion tube study of N2O5 and HONO2 interacting with NaCl and KBr at ambient temperature

ARTICLE *in* PHYSICAL CHEMISTRY CHEMICAL PHYSICS · JUNE 1999

Impact Factor: 4.49 · DOI: 10.1039/A901894H · Source: OAI

3 AUTHORS, INCLUDING:

Michel J Rossi
Paul Scherrer Institut
258 PUBLICATIONS **6,443** CITATIONS

Direct Measurement of Surface Residence Times: Nitryl Chloride and Chlorine Nitrate on Alkali Halides at Room Temperature

Thomas G. Koch and Michel J. Rossi*

Laboratoire de Pollution Atmosphérique (LPA), Ecole Polytechnique Fédérale de Lausanne (EPFL), CH-1015 Lausanne, Switzerland

Received: June 8, 1998; In Final Form: September 1, 1998

To gain quantitative understanding of the "stickiness" of a molecule on a given surface, we have developed a new diffusion tube method that allows us to measure changes in the surface residence times of unreactive as well as reactive adsorbants on solid substrates in real time. The experiment involves sending a pulse of molecules through a tube coated internally with a material of interest. The arrival time of the pulse is recorded using a mass spectrometer, which is mounted at the tube exit in a high vacuum chamber. Since the number of wall collisions under molecular flow conditions is determined only by the tube geometry, the surface residence time can be calculated on a per collision basis. A Monte Carlo simulation, based on the assumption that the molecules are reflected upon collision with a cosine directional distribution, is used to model experimental results. In this study we have measured the surface residence times of two reactive, atmospherically relevant molecules, $ClNO_2$ and $ClONO_2$, on sea-salt aerosol mimics (NaCl, KBr). We found an upper limit of 0.02 ms for the interaction of $ClNO_2$ with KBr and a surface residence time of 0.7 ± 0.2 ms for $ClONO_2$ on NaCl at uptake coefficients of $\gamma = 0.0002$ and 0.1, respectively.

Introduction

Traditionally, heterogeneous interactions at the solid−gas interface have been characterized in terms of reaction probabilities (γ) or accommodation coefficients (α), which can be measured in Knudsen cells operating under molecular flow conditions or in laminar flow tube reactors at pressures of a few Torr.[1−6] Although these techniques have been applied to atmospheric reactions with considerable success, very little can be learned on the length of time a gas molecule resides on the surface before either reaction or desorption occurs. This is mainly due to the fact that these methods routinely employ steady-state conditions integrating the recorded signal over time thereby losing any real-time information of their measurement. However, the surface residence time is a parameter fundamental to the understanding of gas−surface interactions, which could provide additional insight into possible heterogeneous reaction mechanisms, highlighting for instance the role of pore diffusion, the type of bonding involved, etc., particularly where poorly characterized atmospheric substrates, such as soot, sea-salt, or ice, are involved.[7−11]

Heterogeneous chemistry of halogen-containing atmospheric trace gases on sea-salt aerosols has been shown to play a crucial role in the marine boundary layer as it may cause changes in the oxidative capacity of the troposphere.[12] We have therefore looked at potentially relevant reactions of $ClNO_2$, produced via the heterogeneous reaction of N_2O_5 on NaCl, and $ClONO_2$, a abundant reservoir for active chlorine in the stratosphere, which is formed in the gas phase in the presence of NO_x. Either compound can interact with alkali halide surfaces provided by sea-spray aerosols:

$$ClNO_2 + KBr \rightarrow BrNO_2 + KCl \quad (1)$$

$$ClONO_2 + NaCl \rightarrow Cl_2 + NaNO_3 \quad (2)$$

The gaseous products $BrNO_2$ and Cl_2 photolyze readily upon solar irradiation, generating Br and Cl radicals. The latter may react further with hydrocarbons, initiating a chain of oxidation processes in a fashion similar to the OH radical, whereas bromine radicals may catalyze chlorine recycling and contribute to the sudden tropospheric ozone loss phenomenon.[13] The reaction probabilities for reactions 1 and 2 at room temperature have been measured to result in $\gamma = 2 \times 10^{-4}$ and 0.1, respectively.[14,15] These experiments also suggested that nitryl chloride and chlorine nitrate may have significantly different surface residence times on alkali halides despite their similar molecular structure.

The primary aim of this study was to develop and to apply a new technique that enables the first real-time surface residence time measurement of adsorbed gases on unreactive as well as reactive surfaces. We have previously shown that the surface residence time measurement in unreactive cases is reasonably straightforward.[16] For reactive cases the interpretation of data will be based on a simple model of precursor (M_{ads}) to reactive adsorption of a gas molecule (M_g)

$$M(g) \underset{k_{-1}}{\overset{k_1}{\rightleftharpoons}} M(ads) \xrightarrow{k} \text{products} \quad (3)$$

The lifetime (τ) on the surface is given by the inverse of the desorption rate constant plus the heterogeneous loss constant ($1/(k_{-1} + k)$). In this paper we will present four different scenarios for gas−surface interactions: (i) nonreactive nonsticky systems, such as rare gases on Teflon, (ii) nonreactive sticky systems, such as water on Pyrex, (iii) reactive but nonsticky

* To whom correspondence should be addressed.

10.1021/jp982539d CCC: $15.00
Published on Web 10/27/1998

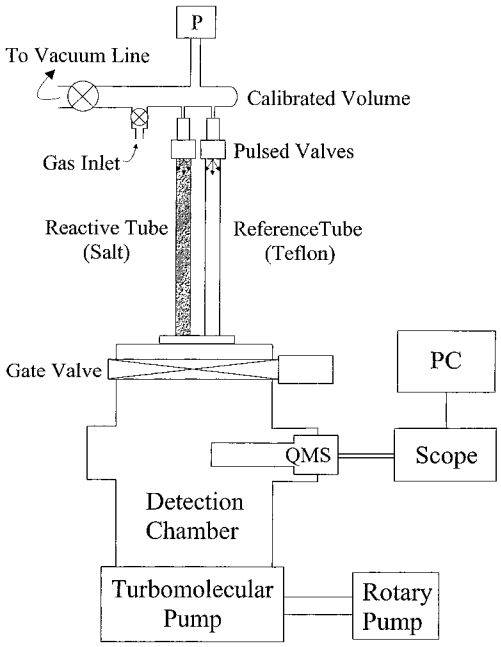

Figure 1. Schematic diagram of the molecular diffusion tube experiment.

systems, such as $ClNO_2$ on KBr, and (iv) reactive sticky systems, such as $ClONO_2$ on NaCl.

Experimental Section

The experiment involves sending a pulse of molecules through a cylindrical reaction tube coated internally with a material of interest, e.g., KBr or NaCl. A second tube coated with Teflon in order to minimize surface interaction serves as a reference. A gas inlet system is mounted at one end of the two tubes and a stainless steel detection chamber at the other end. The detection chamber is equipped with a quadrupole mass spectrometer (Balzers QMS 125, 0−200 amu), which measures the arrival time of the pulse of molecules. It can be isolated from the reactor tubes by a pneumatically operated 6 in. gate valve (VAT, Series 10). To obtain molecular flow conditions, the system is pumped by a turbomolecular pump (Leybold, 360 dm^3 s^{-1}) backed by a rotary pump (Leybold, TRIVAC 16B) reaching a base pressure of less than 1×10^{-8} mbar without bakeout. The vacuum pressure is measured by a hot cathode ionization gauge (Varian 580 Nude Bayard-Albert type). A schematic diagram of the experimental setup is shown in Figure 1.

Standard Pyrex glass tubes served as reactor cylinders, which were thoroughly cleaned before use by rinsing with solvents and a 10% solution of HF in water. The reactive coating was applied by spraying a saturated solution of KBr or NaCl in methanol into the preheated tube (140 °C), which resulted in the condensation of a thin, uniform salt layer. Teflon-coating was carried out in similar fashion using a FEP polymer dispersion (DuPont).[17] To ensure uniform coating for long tubes, multiple sections of 30 cm length were assembled into a single tube. Connections between tube sections were made using greaseless Rotulex joints based on Viton elastomers. Tube dimensions were typically 1−2 cm in diameter and ranged from 20 to 120 cm in length.

Gases were injected from a calibrated volume (ca. 60 cm^3) across a pulsed solenoid valve (General Valve Corporation, Series 9) along the cylinder axis of the tube. The calibrated volume, part of a grease-free gas-handling line, was equipped with a capacitance manometer (MKS Baratron, 0−10 mbar). The number of molecules or atoms per pulse was estimated from the observed pressure drop on the basis of the ideal gas law. Typically, pulses were of millisecond duration corresponding to approximately $(0.2-10) \times 10^{15}$ molecules injected per pulse. Arrival time traces, recorded by mass spectrometer, were displayed and averaged over several pulses using a 500 MHz oscilloscope (Hewlett-Packard, model 54610B) and then transferred to a personal Pentium II computer for kinetic analysis. All experiments were carried out at room temperature.

The arrival time ($t_{arrival}$), defined as the inverse of the decay constant (k) of the time-dependent MS signal, is determined by fitting the measured signal to a single-exponential decay function.

$$t_{arrival} = 1/k \tag{4}$$

Since the experiment operates under molecular flow conditions, i.e., the mean free path of the injected gas molecules is larger than the characteristic tube dimensions, the number of gas−gas collisions is negligible. Hence, the number of collisions inside the reactor tube (Z) only depends on the mass and temperature of the gas injected and on the geometry of the tube.[18,19] The average surface residence time can therefore be calculated directly by comparing the arrival time of an interactive, but nonreactive, gas−surface reaction system ($1/k_{sticky}$) to that of an ideal, that is, noninteractive, system ($1/k_{ideal}$).

$$t_{surf} = \frac{(1/k_{sticky}) - (1/k_{ideal})}{Z} \tag{5}$$

In practice, a Teflon tube serves as a reference for the measurement of k_{ideal}, which has been corrobated by trajectory calculations where the gas−surface interaction has been set to zero. The number of collisions on the inner tube walls (Z) is also computed numerically by a Monte Carlo simulation, which will be described in some detail in the following section.

Monte Carlo Calulations

Monte Carlo trajectory calculations were employed to provide a direct comparison with experimental results.[16,20] The simulation used in this study is based on a Monte Carlo model that has been developed previously in our laboratory to investigate the relationship of gas dynamics and the reactor geometry of Knudsen cells.[6] Using the average molecular velocity, the program calculates the trajectories of individual molecules injected into a given reactor tube geometry on the assumption that the molecules are reflected with a cosine directional distribution upon collision with the wall surface.[21,22] A brief account of the derivation of the algorithm including that for a uniform or $\cos^2$ distribution can be found in the Appendix.

The reactor geometry is modeled by a narrow and a wide cylinder in series, representing the diffusion tube and the detection chamber, respectively. Real tube dimensions are used for the diffusion cylinder whereas the detection chamber, which is 11 dm^3 in volume and contains several blanked off ports, is approximated by a straight cylinder of 12 cm in diameter and 100 cm in length. These dimensions resulted in the best agreement between simulation and experiment if molecules were injected directly into the chamber and the resulting time-dependent MS signal was recorded. The pulsed valve is simulated by a point source located at the geometrical center of the injection plate of the diffusion tube. Individual trajectories are followed by the calculation until the molecule exits from the detection chamber across the pump flange. The total time of a trajectory is saved in a histogram before the next

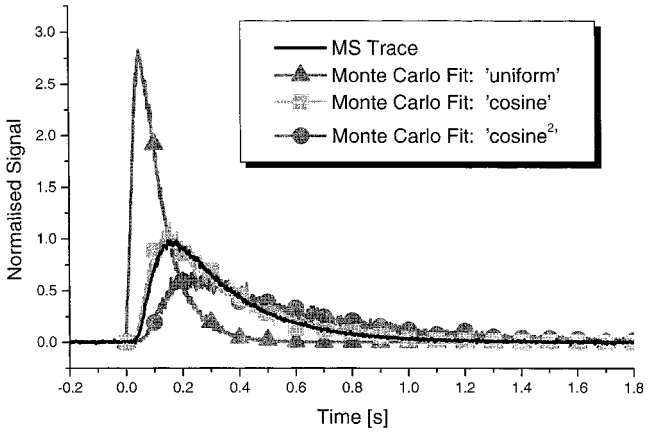

Figure 2. Verification of the algorithm: comparison of the experimentally observed MS signal for noninteractive N_2 molecules passing through a 1.05 × 100 cm tube (Z = 14 000) with Monte Carlo histrograms based on a uniform, cosine and cosine^2 distribution.

molecule is injected. The resulting probability distribution may then be compared directly to the experimentally observed MS trace without making use of any adjustable parameter.

Figure 2 illustrates the verification of the algorithm for the case of a pulse of inert N_2 molecules passing through a 1.05 × 100 cm Pyrex tube: excellent agreement is observed for the experimental MS trace ($1/k_{MS}$ = 0.25 s) with the Monte Carlo histogram based on a cosine directional distribution ($1/k_{cos}$ = 0.26 s). The less directed, uniform or totally random distribution leads to an overestimation of the escape rate constant ($1/k_{uni}$ = 0.08 s) whereas the cosine^2 distribution, which is more directed toward the surface normal, results in an underestimation ($1/k_{cos2}$ = 0.46 s) as the molecules become "stuck" in the tube owing to larger probability of undergoing wall collisions. The statistical error of these measurements is of the order of 10%. It should be noted that we have verified the algorithm further by using different tube geometries[16] and by reproducing literature values reported for transmission probabilities through tubes and orifices.[6]

To model nonideal gases, that is, gases interacting with the wall in a nonreactive manner, an arbitrary surface residence time could be added on a per collision basis. A reaction probability per collision, simulating irreversible heterogeneous loss at the wall surface for reactive gases, may also be introduced. All Monte Carlo programs were written in Fortran and ran on a Pentium personal computer. Typically, 10^4-10^6 trajectories were calculated, taking from a few minutes to more than a day depending on the reactor tube dimensions and the molecular mass of the injected molecule as well as surface residence time and reaction probability.

Other than simulating experimental results, the Monte Carlo approach gives insight into a number of fundamental statistical parameters, such as the average number of collsions in the tube and, more importantly, the integrated collision density, i.e., the total number of collisions per unit surface area. The collisions are by no means distributed evenly along the tube, but the density drops linearly from a maximum value near the injection point to almost zero at the tube exit as demonstrated in Figure 3. The collision frequency, i.e., the number of collisions per unit time, remains the same, however. This may be rationalized most easily by the fact that a molecule near the tube end is more likely to find the exit than a molecule that is located near the injection point. It therefore spends less time in the area near the exit than a molecule close to the injection point. Any

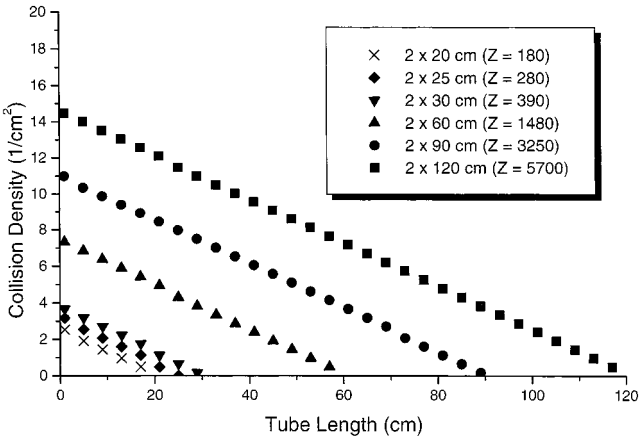

Figure 3. Density of the internal wall collisions along the tube expressed as the integral number of collisions per unit area [1/cm^2].

TABLE 1: Tube Parameters

d (cm)	l (cm)	A (cm^2)	Z_{tube}[a]	$Z_{chamber}$[a]	$1/k$[b] (ms)
2	120	377	5700	130	37.0
2	90	283	3250	130	21.6
2	60	188	1480	130	10.9
2	30	94	390	130	5.9
2	25	79	280	130	5.5
2	20	63	180	130	5.3

[a] Average number of collisions as calculated by the Monte Carlo simulation. [b] Arrival time normalized to 1 amu.

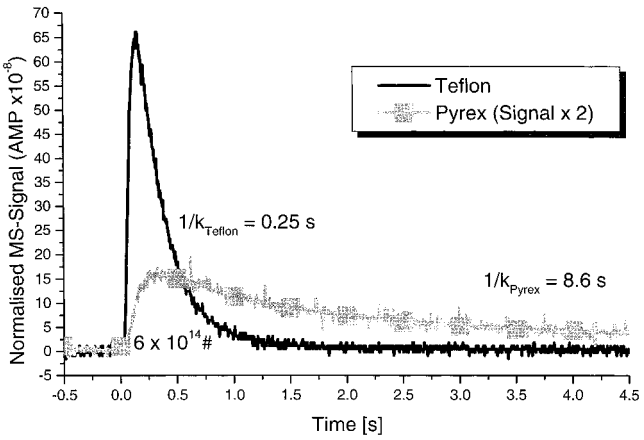

Figure 4. Mass spectrometric signals of a pulse of H_2O molecules (m/e = 18) after passage through a 1.2 × 100 cm tube (Z = 10 000) made of (a) Teflon (PTFE) and (b) Pyrex glass.

saturation effects are therefore most likely to occur near the pulsed valve, particularly in long and narrow tubes. Table 1 summarizes the characteristic parameters of the tubes used in this study.

Results and Discussion

Nonreactive Systems. The high sensitivity of the molecular diffusion tube experiment to gas−surface interactions is demonstrated graphically in Figure 4. It shows a typical, delayed arrival of water vapor passing through a "sticky" Pyrex tube (1.2 × 100 cm) compared to an inert Teflon tube. It is characterized by a longer rise time and slower exponential decay of the mass spectrometric signal compared to the noninteracting case. According to eq 5, which is based on an accommodation coefficient of unity, the late arrival observed for water on Pyrex corresponds to an average surface residence time of 0.84 ms at ambient temperature. The yield of H_2O molecules leaving the

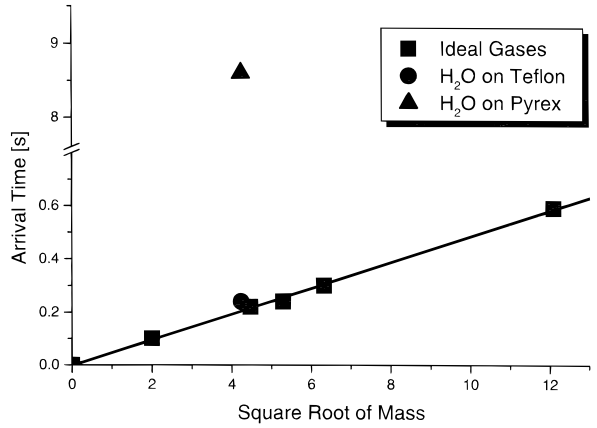

Figure 5. Calibration plot showing the experimental arrival times of a number of ideal gases (He, Ne, N_2, Ar, and SF_6) in a 1.2 × 100 cm tube. The plot also includes the arrival times for water on Teflon as well as on Pyrex glass.

tube is 100%; i.e., irreversible loss of H_2O at the surface does not occur. The yield, or surviving fraction, is determined simply by comparing the integrals of the two MS signals. However, dramatic changes in the adsorption kinetics of water on Pyrex are observed if doses higher than 1×10^{15} molecules per pulse are injected into the 1.2 × 100 cm tube. As we have shown previously,[16] the measured decay signals are no longer single exponential but consist of a fast initial decay, which becomes more pronounced at higher doses, followed by a long "tail", which is largely independent of the dose injected. This is a manifestation of rapid saturation of a limited number of strongly interacting surfaces sites at high exposure. Once these sites are occupied, remaining molecules only find less interactive sites, i.e., sites with shorter surface residence times, which invariably results in faster arrival times. The long tail, which corresponds to the low-dose limit shown in Figure 4, may therefore be interpreted in terms of the desorption of water molecules from the most strongly interacting surface sites. The fact that Pyrex may have a significant amount of water adsorbed to was first demonstrated by Langmuir over 80 years ago.[23]

Whether or not a molecule actually behaves like a rare gas can easily be verified by measuring the arrival times of several rare gases and plotting the values versus the square root of their respective molecular masses. Since the arrival time scales with the inverse of the molecular velocity and thus with the square root of the molecular mass ($\sqrt{M}$), any deviation of $1/k$ from a linear relationship of arrival time vs $\sqrt{M}$ indicates a gas−surface interaction.[16] Figure 5 shows such a calibration plot for a 1.2 × 100 cm tube. The arrival time measured for water vapor on Teflon (0.25s) scales well with the values observed for noninteracting rare gases whereas the arrival time measured for the water/Pyrex system at the low dose limit is more than an order of magnitude larger (8.6 s). Ideal gas behavior on Teflon was also found for other potentially "sticky" gases, such as NO_2 and HCl, confirming the inherent properties of Teflon as a highly inert material. Hence, we use Teflon-coated tubes for all reference measurements.

Reactive, Nonsticky Systems. As a first reactive system we have studied the interaction of $ClNO_2$ with KBr (reaction 1) using three different tube geometries (Z = 1480, 3250, and 5700) and doses ranging from 0.5 to 10×10^{15} molecules per pulse. Mass spectrometric signals were recorded following the ion peaks of the ClN^+ and NO_2^+ fragments at m/e = 49 and 46, respectively. As shown in Table 2, the agreement between the two signals was generally good for all doses and geometries

TABLE 2: Experimental Results for $ClNO_2$ on Teflon and on KBr

surface	tube (cm)	m/e	no.$_{in}$ ($\times 10^{15}$)	no.$_{out}$ (%)[a]	$1/k$ (s)
Teflon	2 × 60	46	0.5	REF	0.092
Teflon	2 × 60	46	1	REF	0.088
Teflon	2 × 60	46	2.5	REF	0.090
Teflon	2 × 60	49	0.5	REF	0.094
Teflon	2 × 60	49	1	REF	0.097
Teflon	2 × 60	49	2.5	REF	0.093
KBr	2 × 60	46	0.5	36.6	0.074
KBr	2 × 60	46	1	37.5	0.073
KBr	2 × 60	46	2.5	45.5	0.074
KBr	2 × 60	49	1	34.8	0.072
KBr	2 × 60	49	2.5	26.7	0.078
KBr	2 × 60	49	5	36.2	0.072
Teflon	2 × 90	46	0.5	REF	0.194
Teflon	2 × 90	46	1	REF	0.197
Teflon	2 × 90	46	2.5	REF	0.204
Teflon	2 × 90	49	0.5	REF	0.199
Teflon	2 × 90	49	1	REF	0.211
Teflon	2 × 90	49	2.5	REF	0.208
Teflon	2 × 90	49	5	REF	0.193
Teflon	2 × 90	49	10	REF	0.199
KBr	2 × 90	46	0.5	15.3	0.139
KBr	2 × 90	46	1	24.6	0.127
KBr	2 × 90	49	1	20.8	0.130
KBr	2 × 90	49	2.5	26.7	0.127
KBr	2 × 90	49	5	27.3	0.130
Teflon	2 × 120	46	0.5	REF	0.334
Teflon	2 × 120	46	1	REF	0.332
Teflon	2 × 120	49	0.5	REF	0.327
Teflon	2 × 120	49	1	REF	0.385
Teflon	2 × 120	49	5	REF	0.351
Teflon	2 × 120	49	10	REF	0.357
KBr	2 × 120	46	1	14.5	0.180
KBr	2 × 120	49	5	17.8	0.136
KBr	2 × 120	49	10	23.6	0.135

[a] The mean values of the yields for each tube geometry are listed in Table 4.

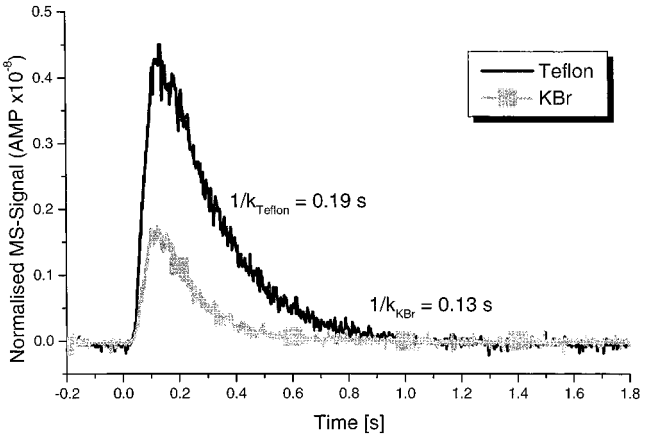

Figure 6. Mass spectrometric signals (m/e = 49) of a pulse of $ClNO_2$ molecules after passage through a 2 × 90 cm tube (Z = 3250) coated with Teflon or KBr.

studied, indicating little or no interference from primary and secondary products, such as $BrNO_2$ and NO_2, which also have mass signals at m/e = 46.[15]

Figure 6 shows a characteristic, time-dependent MS signal of a pulse of $ClNO_2$ molecules effusing out of a 2 × 90 cm tube internally coated with KBr. The arrival time, $1/k$, corresponds to 0.13 s, which is actually *shorter* than that measured using the Teflon reference (0.2 s). On the basis of the integrals under the two signals, the faster arrival time of $ClNO_2$ interacting with KBr is accompanied by a reduction of the surviving fraction

TABLE 3: Arrival Times for $ClNO_2$ Resulting from Monte Carlo Trajectories

mass	tube (cm)	γ	t_{surf} (ms)	yield (%)	$1/k$ (s)
81	2 × 60	0	0	100	0.098
81	2 × 60	0.0001	0	84.4	0.089
81	2 × 60	0.0003	0	67.8	0.080
81	2 × 60	0.001	0	35.2	0.061
81	2 × 90	0	0	100	0.194
81	2 × 90	0.0001	0	70.6	0.153
81	2 × 90	0.0003	0	46.7	0.116
81	2 × 90	0.001	0	15.9	0.068
81	2 × 120	0	0	100	0.333
81	2 × 120	0.0001	0	56.5	0.215
81	2 × 120	0.0003	0	30.8	0.147
81	2 × 120	0.001	0	7.1	0.078

of the injected $ClNO_2$ molecules to 22.9 ± 7.6%. Similar results were obtained for the 2 × 60 and 2 × 120 cm tube. For the former the effect was less pronounced as we observed an average drop in the arrival time from 0.09 s (Teflon) to 0.07 s (KBr, 36.2 ± 9.5% yield), whereas for the latter the changes were considerably more significant with a decrease from 0.35 s (Teflon) to 0.14 s (KBr, 18.7 ± 4.2% yield). No dose dependence was observed so that saturation effects may be excluded. A complete list of all experimental data is presented in Table 2.

From these results it becomes clear that surface residence time analysis for reactive systems, based on the Teflon reference signal alone, is insufficient. Equation 4 is only valid if the gas−surface interaction is temporary and the adsorption fully reversible, i.e. if there is no permanent heterogeneous wall loss. It is imperative to have a closed mass balance for eq 4 to be applicable. Reactive systems therefore pose a new challenge since kinetic analysis is no longer trivial: irreversible uptake of the reactant molecule on the coated diffusion tube walls may lead to an apparent $1/k_{sticky}$ value shorter than $1/k_{ideal}$ owing to the additional heterogeneous loss process. This permanent removal due to heterogeneous reactivity may therefore counteract the "delaying" effect of the molecular surface residence time on the arrival time. To determine the extent of either process, a reliable measurement of the reaction probability is required, which can be achieved by using either mass balance arguments or results of uptake measurements obtained in Knudsen cells. The arrival time signal for a surviving fraction of nonsticky, albeit reactive, molecules may then be calculated using the Monte Carlo simulation, which serves as a reference. Any deviation from the measured signal is then attributed to the surface residence time, which is fitted until good agreement between the calculated and measured traces is obtained.

A modeling study has been carried out in order to demonstrate the effects of a given reaction probability on the arrival time as well as on the surviving fraction for different tube geometries. The results are listed in tabular form in Table 3. The trajectories were calculated for mass 81, facilitating direct comparison of the calculated arrival times to the experimentally observed signals for $ClNO_2$. It immediately becomes obvious that the larger the reaction probability for a given tube the larger the deviation form the "ideal" $1/k$ arrival time value ($\gamma = 0$, or Teflon reference). For a 2 × 90 cm tube the arrival time of $ClNO_2$ drops from 0.09 at $\gamma = 0.0001$ to 0.08 and 0.06 s on increasing the reaction probability by a factor of 3 each time. This phenomenon is even more pronounced for longer tubes as the number of wall collisions increases exponentially with the tube length. Hence, molecules with a given reaction probability are less likely to exit the longer tubes, which is in turn reflected

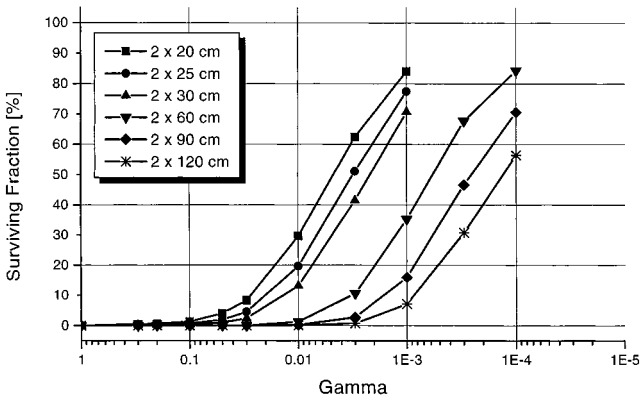

Figure 7. Calibration plot, based on the Monte Carlo method, relating the surviving fraction of the molecule to the reaction probability.

in the yield decreasing significantly with increasing tube length. For example, the yield of $ClNO_2$ molecules exiting a 2 × 120 cm tube at γ values of 0.0001, 0.0003, and 0.001 drops from 57% to 31% and 7%, respectively.

Although the results displayed in Table 3 have been calculated for $ClNO_2$ (mass 81), the yield/reaction probability relationship is in fact inherent to the tube geometry, i.e., independent of the mass of the molecule injected. To be able to relate any measured yield for a given tube geometry to the corresponding reaction probability, we have performed the Monte Carlo simulation systematically over a range of γ values for each tube and constructed a calibration plot as shown in Figure 7. Typically, a 50% yield is obtained for $1/\gamma = Z$, where $1/\gamma$ describes the average number of collsions that lead to a reactive uptake event and Z is the average number of collisions for a particular tube geometry. If $1/\gamma$ becomes smaller than the characteristic value of Z, the surviving fraction asymptotically drops to zero whereas it approaches 100% for $1/\gamma$ values larger than Z. According to this plot, the reaction probability of $ClNO_2$ on KBr is of the order of 0.001 for each of the three tubes. This is approximately a factor of 5 larger than the value found in previous Knudsen cell experiments.[15] Presumably, this discrepancy may in part be due to the relatively large error in our mass balance (Table 4) but also because a certain number of collisions may occur on internal surfaces of the salt layer, which would lead to an overestimation of the reaction probability. For the Monte Carlo calculations we therefore use the value of $\gamma = 0.0002$ obtained by Knudsen cell studies and corrected for pore diffusion.[15]

The time-dependent mass spectrometric signal of $ClNO_2$ propagating across a 2 × 90 cm tube coated with KBr and various Monte Carlo fits are shown in Figure 8. The best agreement between experiment and calculation is observed for the MC histogram based on a γ value of 2×10^{-4} without adding an additional surface residence time. The histogram nicely retraces the rise time as well as the exponential decay of the observed MS signal. If a surface residence time as small as 200 or even 50 μs is added, the agreement becomes worse: the maximum of the arrival time histogram is shifted to longer times, and the exponential decay becomes slower. Using the 2 × 120 tube, which is the most sensitive to weak gas−surface interactions owing to the highest number of collisions, we have determined an upper limit of the surface residence time of 20 μs. In other words, the $ClNO_2$ on KBr behaves like a reactive, but nonsticky gas. A summary of the surface residence time measurements including uncertainties for all the reactor geometries used is presented in Table 4.

TABLE 4: Summary of Combined $ClNO_2$ Results

tube (cm)	Z	surface	$no._{in}$ ($\times 10^{15}$)	$no._{out}$ (%)	$1/k$ (s)	γ	t_{surf} (ms)
2×60	1480	Teflon	0.5−2.5	REF	0.092 ± 0.01		
2×60	1480	KBr	0.5−5	36.2 ± 9.5	0.074 ± 0.08	2×10^{-4}	< 0.04
2×90	3250	Teflon	0.5−10	REF	0.201 ± 0.02		
2×90	3250	KBr	0.5−5	22.9 ± 7.6	0.131 ± 0.02	2×10^{-4}	< 0.03
2×120	5700	Teflon	0.5−10	REF	0.348 ± 0.04		
2×120	5700	KBr	1−10	18.7 ± 4.2	0.150 ± 0.03	2×10^{-4}	< 0.02

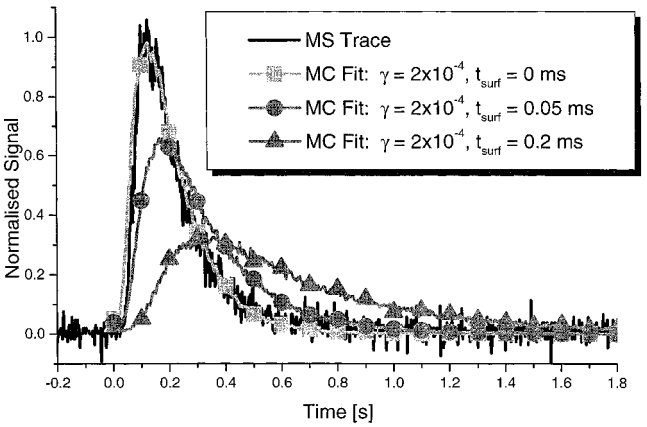

Figure 8. Monte Carlo fits for $ClNO_2$ propagating through a 2×90 cm tube ($Z = 3250$) coated with KBr.

Reactive, Sticky Systems. A similar series of experiments was carried out for $ClONO_2$ on NaCl. However, owing to the considerably higher reaction probability ($\gamma = 0.1$), much shorter diffusion tubes had to be used in order to ensure a surviving fraction of molecules large enough to be measured. Tube geometries therefore ranged from 2×20 cm ($Z = 180$) to 2×30 cm ($Z = 390$), and doses were typically of the order of $(1-10) \times 10^{15}$ molecules per pulse. Mass spectrometric signals were recorded following the signals at $m/e = 51$ and 46, corresponding to the ClO^+ and NO_2^+ fragments, respectively. Any discrepancies between the 51 and 46 signals are largely due to the fact that a small amount $ClONO_2$ decomposes by reacting with residual H_2O adsorbed on the reactor walls producing HOCl, which itself exhibits a strong signal at $m/e = 51$. Hence, most measurements were taken at m/e 46. The contribution of the potential trace impurity nitric acid to the $m/e = 46$ signal is thought to be neglible on the basis of reference experiments we have carried out. A single NaCl coating could be used for several experiments if low doses of $ClONO_2$ were injected. A complete list of all experimental data is shown in Table 5.

The experimental MS signals of a pulse of $ClONO_2$ molecules passing through a 2×20 cm tube coated with Teflon or NaCl are shown in Figure 9. On the basis of the difference of the two integrals, only $5.0 \pm 2.4\%$ of the injected $ClONO_2$ molecules survive the Z collisions in the NaCl coated tube owing to the large reaction probability ($\gamma = 0.1$) obtained in Knudsen cell experiments.[15] As outlined above, rapid heterogeneous wall loss usually results in a faster decay constant. However, the arrival time actually measured for $ClONO_2$ on NaCl (0.049 ± 0.005 s) is longer than that for $ClONO_2$ interacting with Teflon (0.023 ± 0.003 s). This clearly suggests a significant surface residence time, which, from a purely kinetic point of view, counteracts and even overcompensates the "accelerating" effect of the reactive uptake on the arrival time. At high doses, i.e., repeated exposure of the NaCl surface to pulses of 10^{16} molecules, we observed a shortening of the arrival time from 0.049 ± 0.005 s to 0.026 ± 0.003 s, which was accompanied by an increase of the surviving fraction of molecules from approximately 5.0% to 19.8%. Presumably, this is due to the formation $NaNO_3$ on the surface, which is unreactive toward $ClONO_2$ and decreases the gas−surface interaction. The majority of experiments was therefore carried out in the low-exposure regime.

TABLE 5: Experimental Results for $ClONO_2$ on Teflon and on NaCl

surface	tube (cm)	m/e	$no._{in}$ ($\times 10^{15}$)	$no._{out}$ (%)	$1/k$ (s)
Teflon	2×20	51	1	REF	0.021
Teflon	2×20	46	0.5	REF	0.023
Teflon	2×20	46	1	REF	0.023
Teflon	2×20	46	1	REF	0.022
Teflon	2×20	46	2.5	REF	0.023
Teflon	2×20	46	10	REF	0.023
NaCl	2×20	51	1	10.2	0.031
NaCl	2×20	46	0.5	6.2	0.050
NaCl	2×20	46	1	3.5	0.052
NaCl	2×20	46	1	5.8	0.046
NaCl	2×20	46	2.5	4.5	0.047
NaCl	2×20	46	10[a]	5.1	0.050
NaCl	2×20	46	10[a]	6.4	0.048
NaCl	2×20	46	10[a]	7.1	0.047
NaCl	2×20	46	10[a]	16.0	0.031
NaCl	2×20	46	10[a]	19.8	0.026
Teflon	2×25	46	1	REF	0.029
Teflon	2×25	51	1	REF	0.024
NaCl	2×25	46	1	5.8	0.046
NaCl	2×25	46	2.5	5.7	0.044
NaCl	2×25	51	1	14.1	0.040
NaCl	2×25	51	1	17.7	0.046
NaCl	2×25	51	2.5	31.8	0.044
Teflon	2×30	46	1	REF	0.038
Teflon	2×30	51	1	REF	0.033
NaCl	2×30	46	1	4.2	0.057
NaCl	2×30	51	1	8.9	0.059

[a] Repeated exposure of a NaCl coating to high doses of $ClONO_2$.

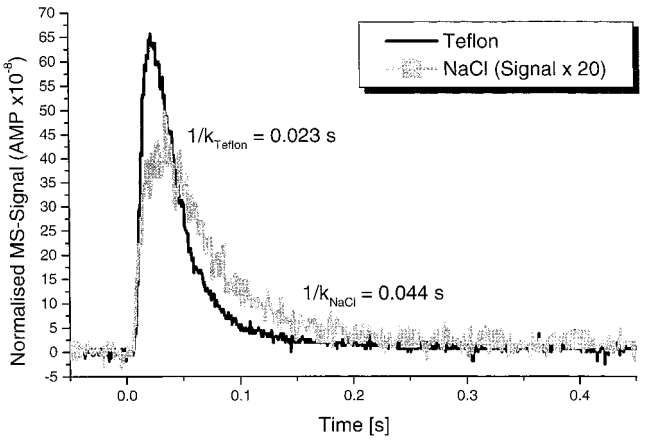

Figure 9. Mass spectrometric signals ($m/e = 46$) of a pulse of $ClONO_2$ molecules after passage through a 2×20 cm tube ($Z = 280$) coated with Teflon or NaCl.

The Monte Carlo results for $ClONO_2$ are summarized in Table 6. The arrival times calculated for the Teflon reference signals ($\gamma = 0$, $t_{surf} = 0$) for each of the three tube geometries appear

TABLE 6: Arrival Times for $ClONO_2$ Resulting from Monte Carlo Trajectories

mass	tube (cm)	γ	t_{surf} (ms)	yield (%)	1/k (s)
97	20	0	0	100	0.052
97	20	0.1	0	1.3	0.045
97	20	0.1	0.5	1.3	0.046
97	20	0.1	1	1.3	0.050
97	20	0.1	2	1.3	0.054
97	20	0.05	0	3.8	0.048
97	20	0.05	0.5	3.8	0.049
97	20	0.05	1	3.8	0.056
97	20	0.05	2	3.8	0.072
97	25	0	0	100	0.054
97	25	0.1	0	0.64	0.049
97	25	0.1	0.5	0.64	0.048
97	25	0.1	1	0.64	0.055
97	25	0.1	2	0.64	0.063
97	30	0	0	100	0.058
97	30	0.1	0	0.37	0.047
97	30	0.1	0.5	0.37	0.057
97	30	0.1	1	0.37	0.070
97	30	0.1	2	0.37	0.081

to be larger by a factor of 2 compared to the corresponding experimental values, whereas the yields for reactive uptake calculated in the simulation appear to be systematically lower (Table 5). This discrepancy strongly suggests a partial decomposition of the highly reactive $ClONO_2$ molecules in the reference tube, presumably on imperfections in the Teflon coating or on the stainless steel walls of the detection chamber. A reference yield of less than 100% would inevitably lead to an overestimation of the yield of the reactive uptake studied in the reaction tube, which in turn would lead to too low a reaction probability using the calibration plot shown in Figure 7. We have therefore used the Knudsen cell value of $\gamma = 0.1$ in the Monte Carlo fits.[15]

Monte Carlo histograms for $ClONO_2$ molecules with various surface residence times undergoing reactive uptake ($\gamma = 0.1$) in a 2 × 20 cm tube ($Z = 280$) are shown Figure 10. Unlike the simulations shown in Figure 8 for the reactive uptake of $ClNO_2$, which exhibit a smooth rise and decay signal, the calculated signals for $ClONO_2$ are characterized by a strong initial spike, followed by a second, broader and less intense peak that trails off in a single-exponential decay. The position of the initial spike remains relatively constant over the range of surface residence times studied, whereas the second maximum is strongly dependent on the surface residence added as it shifts to longer arrival times at longer surface residence times. The integral remains the same since it is determined by the reaction probability. Analysis of individual trajectories in the Monte Carlo simulation shows that the initial peak corresponds to molecules that undergo very few or no collisions at all in the tube so that the arrival time is principally determined by the molecular trajectory and not by the surface residence time. Although this phenomon plays an integral part in relation to the signal rise time in general, the high intensity and clear distinction from the subsequent decay curve in this case is related to the extremely low probability of molecules undergoing many collisions and then exiting the tube: on average every 10th collision leads to irreversible uptake whereas typically 280 collisions are needed to find the tube exit. The observed histogram therefore primarily consists of molecular trajectories having undergone of the order of 10 or less collisions, i.e., an initial spike, which carries little information on the surface residence time. The reason this artifact does not show up in the experimentally measured MS signal is most likely due to the finite response time of the mass spectrometer, particularly

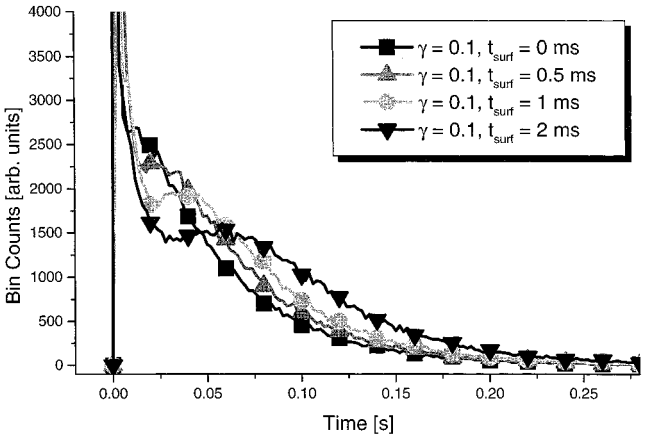

Figure 10. Monte Carlo histograms for $ClONO_2$ molecules undergoing reactive uptake in a 2 × 20 cm tube ($Z = 280$).

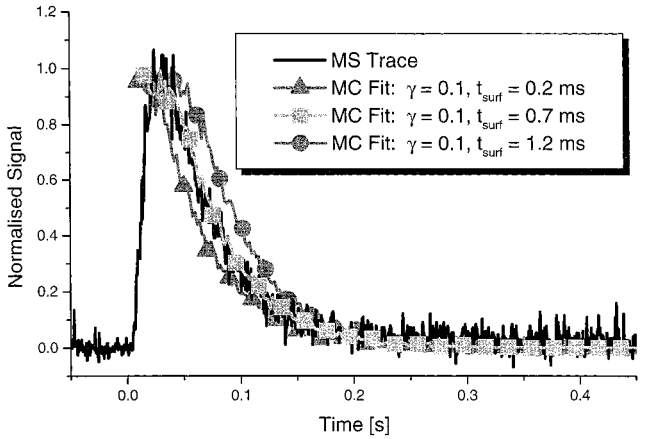

Figure 11. Monte Carlo fits for $ClONO_2$ propagating though a 2 × 20 cm tube ($Z = 280$) coated with NaCl.

at the large amplifications needed to detect the low yield of surviving $ClONO_2$ molecules. The complicated shape of the detection chamber may also contribute to a spread of arrival times larger than that calculated by the simulation. Hence, we only fit the second maximum and exponential decay of the Monte Carlo histogram to the observed MS signal, as it corresponds to the fraction of molecules for which the arrival time is governed by the surface residence time.

Figure 11 shows various Monte Carlo fits for a pulse of $ClONO_2$ molecules passing through a 2 × 20 cm tube coated with NaCl. The Monte Carlo histograms were calculated for a reaction probability of $\gamma = 0.1$ using a surface residence time of 0.2, 0.7, and 1.2 ms to demonstrate the accuracy of the fit. The best agreement was observed for $t_{surf} = 0.7$ ms with an error limit of ±0.2 ms. The calculated portion of the rise of the signal was omitted for reasons of clarity. We have confirmed the results of the 2 × 20 cm tube using a 2 × 25 and 2 × 30 cm tube, measuring a surface residence time of 1.0 ± 0.4 and 1.2 ± 0.5 ms, respectively. A summary of all results is listed in Table 7. For the highly reactive chlorine nitrate on NaCl, the statistical error increases with tube length due to a smaller signal-to-noise ratio caused by the lower number of molecules leaving the tube. In fact, we were unable to measure the surface residence time of $ClONO_2$ on KBr because of the even larger reactivity ($\gamma = 0.3$). It should be noted that the uncertainty of the measurement may also increase if the tube is too short since there are insufficient wall collisions to differentiate the signal obtained in the coated tube from the reference

TABLE 7: Summary of Combined $ClONO_2$ Results

tube (cm)	Z	surface	no.$_{in}$ ($\times 10^{15}$)	no.$_{out}$ (%)	$1/k$ (s)	γ	t_{surf} (ms)
2×20	180	Teflon	1−10	REF	0.023 ± 0.002		
2×20	180	KBr	1−10	5.0 ± 2.6	0.049 ± 0.005	0.1	0.7 ± 0.2
2×25	280	Teflon	1−2.5	REF	0.027 ± 0.003		
2×25	280	KBr	1−2.5	5.8 ± 2.7	0.044 ± 0.005	0.1	1.0 ± 0.4
2×30	390	Teflon	1	REF	0.035 ± 0.004		
2×30	390	KBr	1	4.2 ± 2.4	0.057 ± 0.006	0.1	1.2 ± 0.5

TABLE 8: Relevant Equations for Different Directional Distribution Functions

distribution	uniform	cosine	cosine^2
1d-DDF	$I = I_0\, d\Omega$	$I = I_0 \cos\theta\, d\Omega$	$I = I_0 \cos^2\theta\, d\Omega$
3d-DDF	$I = 2\pi R^2 I_0 \sin\theta\, d\varphi$	$I = 2\pi R^2 I_0 \cos\theta \sin\theta\, d\varphi$	$I = 2\pi R^2 I_0 \cos^2\theta \sin\theta\, d\varphi$
F[a]	$F = 1 - \cos\theta$	$F = \sin^2\theta$	$F = 1 - \cos^3\theta$
algorithm	$\theta = \arccos(\mathrm{RNUM})$	$\theta = \arcsin(\sqrt{\mathrm{RNUM}})$	$\theta = \arccos(3\sqrt{\mathrm{RNUM}})$

[a] Fraction of all molecules emitted for all angles less or equal to θ.

signal. We are currently building a second apparatus with a smaller detection chamber in order to increase our sensitity further when using short tubes and highly reactive systems.

Conclusion

The primary aim of this study was to develop and apply a novel technique that enables the first real-time surface residence time measurement of adsorbates on unreactive as well as reactive substrates. We have presented four different scenarios for the diffusion of gases through tubes: (i) ideal gases, (ii) sticky but unreactive gases, such as H_2O on Pyrex, (iii) nonsticky but reactive gases, such as $ClNO_2$ on KBr, and (iv) sticky reactive gases, such as $ClONO_2$ on NaCl. For unreactive gases, the surface residence can be measured analytically whereas modeling is required for reactive systems. Our results show that the surface residence time of the highly reactive $ClONO_2$ on NaCl ($\gamma = 0.1$; $t_{surf} = 0.7$ ms) is at least 30 times larger than that of the much less reactive $ClNO_2$ on KBr ($\gamma = 2 \times 10^{-4}$; $t_{surf} < 30\ \mu$s), which is presumably due to a strong $Cl^- \cdots {}^{\delta+}ClONO_2$ interaction. This clearly suggests that long surface residence times pertaining to sticky molecules may be related to high uptake probabilities.

Although the case of $ClONO_2$ may also serve to highlight the inherent limitations of the technique for the study of very reactive molecules, we have shown that the molecular diffusion tube is a poweful tool to measure surface residence times, particularly where unreactive and slowly reacting systems ($\gamma < 0.01$) are concerned. This novel technique may therefore be employed on a routine basis along with Knudsen cells and flow tubes in order to determine the extent of any heterogeneous interaction at the gas−solid interface.

Acknowledgment. This work has been funded by the Fonds National Suisse (FNS) and the Office Fédéral de l'Enseignement et de la Science (OFES) as part of the subproject HALOTROP of the EC Environment and Climate Programme. We also thank Professor Hubert van den Bergh for his lively interest.

Appendix

The algorithm used in the Monte Carlo simulation, relating a random number to a cosine directional distribution, is briefly derived in the following. The one-dimensional directional distribution function (1d-DDF) for the cosine law of molecular emission is expressed mathematically as

$$I = I_0 \cos\theta\, d\Omega \tag{A1}$$

where I is the molecular flow through the differential solid angle $d\Omega$, I_0 the flux in the direction of the surface normal, and θ the angle of $d\Omega$ to the surface normal. To find the desired three-dimensional distribution function of molecular emission (3d-DDF) we use

$$d\Omega = R\, d\theta\, R \sin\theta\, d\varphi \tag{A2}$$

and integrate from 0 to 2π resulting in

$$I = 2\pi R^2 I_0 \cos\theta \sin\theta\, d\theta \tag{A3}$$

The fraction (F) of all molecules emitted for all angles less or equal to θ is obtained by integrating eq A3 from 0 to θ and dividing by the total number of molecules emitted:

$$F = \sin^2\theta \tag{A4}$$

Hence, the appropriate equation for relating the angle θ to the random number (RNUM) selected over the interval [0, 1] is given by

$$\theta = \arcsin(\sqrt{\mathrm{RNUM}}) \tag{A5}$$

The derivations of the three-dimensional uniform and cosine^2 directional distributions are carried out accordingly. The relevant equations are summarized in Table 8.

A second random number, evenly distributed over the interval $[0, 2\pi]$, is required to find the orientation within the emission cone described by eq A1. Once the two angles are selected the next impact location due to wall collision may be calculated using the average molecular velocity (c)

$$c = \sqrt{\frac{8RT}{\pi M}} \tag{A5}$$

as the vector for the trajectory, where R is the ideal gas constant, T the temperature, and M the molecular mass of the molecule.

References and Notes

(1) Molina, M. J.; Molina, L. T.; Golden, D. M. *J. Phys. Chem.* **1996**, *12*, 12888.

(2) Kolb, C. E.; Worsnop, D. R.; Zahniser, M. S.; Davidovits, P.; Keyser, C. F.; Leu, M. T.; Hanson, D. R.; Ravishankara, A. R.; Williams, L. R.; Tolbert, M. A. Progress and Problems in Atmospheric Chemistry. In *Advances in Physical Chemistry Series;* Barker, J. R., Ed.; World Scientific Publishing: River Edge, NJ, 1995; Vol. 3, pp 771−875.

(3) Golden, D. M.; Spokes G. N.; Benson, S. W. *Angew. Chem., Int. Ed. Engl.* **1973**, *12*, 534.

(4) Rossi, M. J.; King, K. D.; Golden, D. M. *J. Am. Chem. Soc.* **1979**, *101*, 1223.

(5) Caloz, F.; Fenter, F. F.; Tabor, K.; Rossi, M. J. *Rev. Sci. Instrum.* **1997,** *68*, 3172.
(6) Fenter, F. F.; Caloz, F.; Rossi, M. J. *Rev. Sci. Instrum.* **1997,** *68*, 3180.
(7) Keyser, L. F.; Moore, S. B.; Leu, M. T. *J. Phys. Chem*. **1991**, *95*, 5496.
(8) Koch, T. G.; Banham, S. F.; Sodeau, J. R.; Horn, A. B.; McCoustra, M. R. S.; Chesters, M. A. *J. Geophys. Res*. **1997**, *D102*, 1513.
(9) Gertner, J. B.; Hynes, J. T. *Science* **1996**, *271*, 1563.
(10) Tabor, K.; Gutzwiller, L.; Rossi, M. J. *J. Phys. Chem*. **1994**, *98*, 6172.
(11) Eichler, B.; Baltensperger, U.; Ammann, M.; Jost, D. T.; Gäggeler, H.-R.; Türler, A. *Radiochim. Acta* **1995**, *68*, 41.
(12) Versino, B. The Oxidising Capacity of the Troposphere. *Proceedings of the Seventh European Symposium*, Venice, Italy, 2−4 October, 1996; The European Commission: B-1049 Brussels, 1996.
(13) Platt, U.; Lehrer, E. *Arctic Tropospheric Ozone Chemistry*; Air Pollution Research Report No. 64, EUR 17783; The European Commission: B-1049 Brussels, 1997.
(14) Caloz, F.; Fenter, F. F.; Rossi, M. J. *J. Phys. Chem*. **1996**, *100*, 7496.
(15) Caloz, F.; Seisel, S.; Fenter, F.; Rossi; M. J. *Submitted to J. Phys. Chem*.
(16) Koch, T. G., Fenter, F. F.; Rossi, M. J.; *Chem. Phys. Lett*. **1997**, *275*, 253.
(17) *Teflon FEP 120 Information Brochure*, Du Pont de Nemours International S.A., Division Fluoropolymères, CH-1211 Geuève (Suisse), 1984.
(18) Dushman, S. *Scientific Foundations of the Vacuum Technique*, 2nd ed.; John Wiley and Sons: New York, 1961.
(19) Steckelmacher, W. *Rep. Prog. Phys*. **1986**, *49*, 1083.
(20) Benck, R. F.; Ward, J. W.; Bloore, E. *J. Vac. Sci. Technol*. **1969**, *7*, 403.
(21) Levenson, L. L.; Milleron, N.; Davis, D. H. *Le Vide* **1963**, *103*, 42.
(22) Boeckmann, M. D. *J. Vac. Sci. Technol*. **1986**, *A4*, 353.
(23) Langmuir, I. *J. Chem. Am. Soc*. **1918,** *40*, 1361.